Low-Spin Tris(quinone oximates) of Manganese(II,III). Synthesis, Isomerism, and Equilibria†

Partha Basu and Animesh Chakravorty*

Department of Inorganic Chemistry, Indian Association for the Cultivation of Science, Calcutta 700 032, India

Received February 6, 1992

The manganese(III) tris chelates $Mn(RQ)_3$ (**1**, R = Cl, Br, Me, ^{t}Bu) synthesized from 1,2-quinone oximes (HRQ) and $Mn(MeCO_2)_3\cdot 2H_2O$ are low spin ($S = 1$, 2.9–3.1 μ_B at 298 K) both in the solid state and in solution. Their *mer* geometry is proven by ^{1}H NMR spectra in $CDCl_3$ solution. The manganate(II) anions, $Mn(RQ)_3^-$, have been electrogenerated in solution from $Mn(RQ)_3$ and are uniformly low spin ($S = {}^1/_2$, 1.8–2.0 μ_B at 298 K). The salt $[Et_4N][Mn(ClQ)_3]$ (1.77 μ_B at 298 K) has been isolated and structurally characterized: chemical formula $C_{26}H_{29}N_4O_6Cl_3Mn$; crystal system triclinic; space group $P\bar{1}$; a = 12.205 (6) Å, b = 13.645 (9) Å, c = 18.076 (10) Å; α = 91.04 (5)°, β = 94.07 (4)°, γ = 96.06 (4)°; V = 2985 (3) Å^3; Z = 4; R = 8.80%, R_w = 8.88%. The lattice consists of an ordered arrangement of equal proportions of *mer* and *fac* isomers. The average Mn–O and Mn–N distances are 1.97 (1) and 1.93 (2) Å, respectively. Isomer-specific nonbonded Cl···Cl interactions are important in crystal packing. Variable-temperature voltammetry of $Mn(RQ)_3^-$ has revealed the presence of isomeric equilibria in solution—the equilibrium constant K^{II} (=[*mer*]/[*fac*]) lying in the range 2–3 at 260 K in dichloromethane. On the other hand, the electrochemistry of $Mn(RQ_3)$ is consistent with the virtually exclusive presence of the *mer* isomer. The equilibrium constant K^{III} (=[*mer*]/[*fac*]) for $Mn(RQ)_3$ has been estimated to be $\sim 10^4$ at 260 K in dichloromethane. The unstable *fac*-$Mn(RQ)_3$ isomer can be observed by stereoretentive voltammetry of the *fac–mer* equilibrium mixture of $Mn(RQ)_3^-$. It spontaneously isomerizes with a rate constant of $\sim$0.03 s^{-1} (260 K, dichloromethane). The manganese(III)–manganese(II) formal potentials are isomer dependent, and for a given R, $E°(fac)$ is 170–180 mV more positive than $E°(mer)$. The inequalities $K^{III} > K^{II}$ and $E°(fac) > E°(mer)$ are thermodynamically interrelated, and some of the factors controlling them are examined.

Introduction

Quinone oxime tris chelates of type **1** incorporating 3d elements have been of interest to us.[1-3] The biological pigment ferroverdin

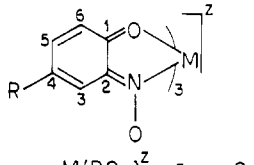

$M(RQ_3)^z$, z = −, 0

1

has the chromophore $Fe^{II}(RQ)_3^-$, R = *p*-$(CH_2{=}CH)$-$C_6H_4OC(=O)$.[4-6] Synthetic (R = Me, Cl, etc.) ferroverdins (z = 1−) and ferriverdins (z = 0), $Fe(RQ)_3^z$, are low spin and display *fac–mer* isomerism.[1,2] This has prompted us to examine their manganese analogs as part of our program on the chemistry of MnO_nN_{6-n} species.[7-11] A strong motivating factor has been the prospect of observing situations that are rare for di- and trivalent manganese: low-spin configuration and tris chelate geometrical isomerism.

The synthesis and characterization of a group of $Mn(RQ)_3^z$ (z = 1−, 0) complexes are described.[12,13] Geometrical isomerism is observed. Both oxidation states are low spin, but the isomer preferences of the two states are very different. Spontaneous isomerization occurs upon metal redox. The z = 0/1− reduction potentials are isomer dependent. The observed trends have been qualitatively rationalized. A remarkable crystalline $Mn(RQ)_3^-$ structure in which *mer* and *fac* isomers coexist in an ordered 1:1 proportion has been isolated and structurally characterized.

Results and Discussion

A. Synthesis. The HRQ ligands (R = Cl, Br, Me, ^{t}Bu) used in the present work were obtained as unstable orange-yellow solids by the Baudisch–Cronheim reaction, i.e., nitrosation of phenols in the presence of copper(II) followed by acid decomposition of the $Cu(RQ)_2$ complex so formed.[14] The reaction of HRQ with manganese(III) acetate in methanol afforded $Mn^{III}(RQ)_3$ in excellent yield as a dark-colored solid. The electronic spectrum

† Dedicated to Professor Frank Albert Cotton on the occasion of his 62nd birthday.

(1) Basu, P.; Choudhury, S. B.; Pal, S.; Chakravorty, A. *Inorg. Chem.* **1989**, *28*, 2680–2686.
(2) (a) Basu, P.; Pal, S.; Chakravorty, A. *J. Chem. Soc., Chem. Commun.* **1989**, 977–978. (b) Chattopadhyay, S.; Basu, P.; Ray, D.; Pal, S.; Chakravorty, A. *Proc. Indian Acad. Sci. (Chem. Sci.)* **1990**, *102*, 195–202.
(3) Ray, D.; Chakravorty, A. *Inorg. Chem.* **1987**, *27*, 3292–3297.
(4) (a) Chain, E. B.; Tonolo, A.; Carilli, A. *Nature* **1955**, *176*, 645. (b) Ehrenberg, A. *Nature* **1956**, *178*, 379–380. (c) Ballio, A.; Bertholdt, H.; Chain, E. B.; Vittorio, V. D. *Nature* **1962**, *194*, 769–770. (d) Ballio, A.; Bertholdt, H.; Carilli, A.; Chain, E. B.; Vittorio, V. D.; Tonolo, A.; Vero-Bercellona, L. *Proc. R. Soc. London, B* **1963**, *158*, 43–70. (e) Neilands, J. B. *Struct. Bonding* **1966**, *1*, 59–108.
(5) (a) Candeloro, S.; Grdenic, D.; Taylor, N.; Thompson, B.; Viswamitra, M.; Hodgkin, D. C. *Nature* **1969**, *224*, 589–591. (b) Ballio, A.; Barcellona, S.; Chain, E. B.; Tonolo, A.; Vero-Bercellona, L. *Proc. R. Soc. London, B* **1964**, *161*, 384–391.
(6) Basu, P.; Pal, S.; Chakravorty, A. *J. Chem. Soc., Dalton Trans.* **1990**, 9–11.
(7) Chandra, S. K.; Basu, P.; Ray, D.; Pal, S.; Chakravorty, A. *Inorg. Chem.* **1990**, *29*, 2423–2428.
(8) (a) Chandra, S. K.; Choudhury, S. B.; Ray, D.; Chakravorty, A. *J. Chem. Soc., Chem. Commun.* **1990**, 474–475. (b) Chandra, S. K.; Chakravorty, A. *Inorg. Chem.* **1992**, *31*, 760–765.
(9) Dutta, S.; Basu, P.; Chakravorty, A. *Inorg. Chem.* **1991**, *30*, 4031–4037.
(10) Chandra, S. K.; Chakravorty, A. *Inorg. Chem.* **1991**, *30*, 3795–3796.
(11) (a) Chattopadhyay, S.; Basu, P.; Pal, S.; Chakravorty, A. *J. Chem. Soc., Dalton Trans.* **1990**, 3829–3833. (b) Basu, P.; Pal, S.; Chakravorty, A. *Inorg. Chem.* **1988**, *27*, 1848–1850.
(12) Manganese(III) tris chelates of naphthoquinone oximes have been reported to be catalysts for olefin epoxidation, but no other properties have been reported: Balauch, D.; Charalambous, J.; Haines, L. I. B. *J. Chem. Soc., Chem. Commun.* **1988**, 1178–1179.
(13) Some bis chelates of manganese(II) are known:[12] Gurrieri, S.; Siracusa, G. *Inorg. Chim. Acta* **1971**, *5*, 650–654.
(14) (a) Baudisch, O. *Science* **1940**, *92*, 336–337. (b) Cronheim, G. *J. Org. Chem.* **1947**, *12*, 1–29.

0020-1669/92/1331-4980$03.00/0

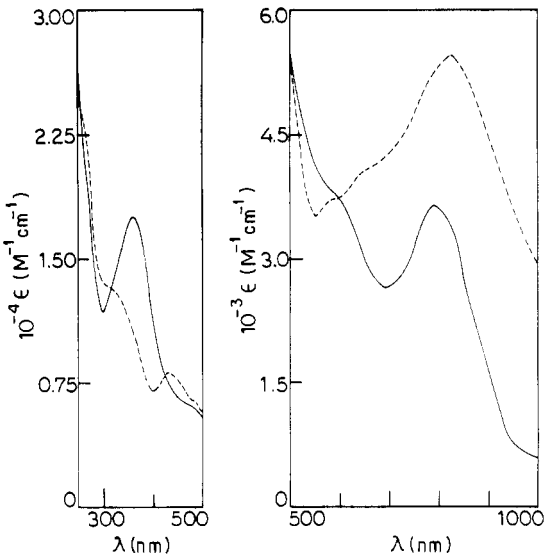

Figure 1. Electronic spectra of $Mn(ClQ)_3$ (—) in CH_2Cl_2 and $[Et_4N][Mn(ClQ)_3]$ in MeCN (- - -) at 298 K.

Table I. Magnetic Data for $Mn(RQ)_3^z$ Complexes at 298 K

complex	μ_{eff}, μ_B in solid	μ_{eff}, μ_B in soln[a]	complex[b]	μ_{eff}, μ_B in soln[c]
$Mn(ClQ)_3$	2.98	3.10	$Mn(ClQ)_3^-$	1.80[d]
$Mn(BrQ)_3$	2.95	3.05	$Mn(BrQ)_3^-$	1.85
$Mn(MeQ)_3$	2.95	3.00	$Mn(MeQ)_3^-$	2.00
$Mn(^tBuQ)_3$	2.92	2.97	$Mn(^tBuQ)_3^-$	1.87

[a] In chloroform. [b] Generated by bulk electrolysis. [c] In dichloromethane. [d] In solid $[Et_4N][Mn(ClQ)_3]$, the magnetic moment is 1.77 μ_B.

of $Mn(ClQ)_3$ shown in Figure 1 is representative of the family. Analytical data for $Mn(RQ)_3$ have been deposited as supplementary material (Table SI).

The reaction of HRQ with manganese(II) salts affords intractable mixtures of species. However, green $Mn^{II}(RQ)_3^-$ can be quantitatively generated in solution from $Mn(RQ)_3$ via electrolytic reduction; vide infra. The salt $[Et_4N][Mn(ClQ)_3]$ has been isolated in the pure state by this route. The electronic spectrum of $Mn(ClQ)_3^-$ is shown in Figure 1.

B. Low-Spin Configuration. a. Magnetic Data. The magnetic moments of $Mn(RQ)_3$ species lie near 3 μ_B both in the solid state and in solution (Table I). The complexes are thus low spin with incompletely quenched orbital moments (t_2^4, $S = 1$; spin-only moment 2.83 μ_B). The status of $Mn(RQ)_3^-$ is similar (t_2^5, $S = {}^1/_2$). The moment of solid $[Et_4N][Mn(ClQ)_3]$ and the moments of all the $Mn(RQ)_3^-$ species in solution lie in the range 1.8–2.0 μ_B (Table I). The $Mn(RQ)_3$ complexes are EPR-silent but display paramagnetically shifted ^1H NMR spectra; vide infra. On the other hand, dichloromethane solutions of $Mn(RQ)_3^-$ afford well-resolved EPR spectra with six ^{55}Mn hyperfine lines[15] ($g = 2.026$–2.028; $A = 95$–97 G).

Very few low-spin complexes of di- and trivalent manganese are currently known: manganese(III) in cyano and porphyrinato complexes[16-18] and manganese(II) in cyano[19-20] and carbonyl phosphine[21] complexes as well as in the tris chelates **2**[11] and **3**.[22]

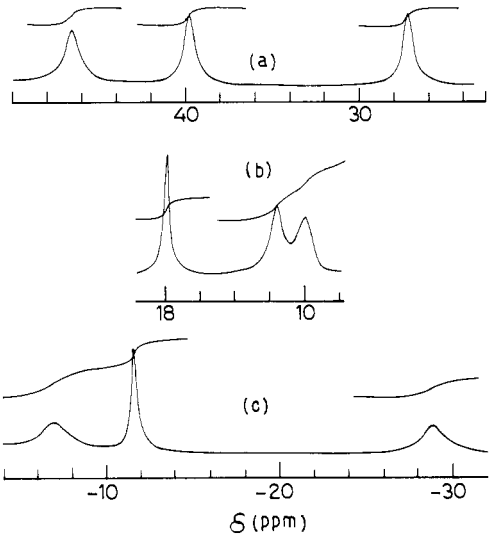

Figure 2. 270-MHz ^1H NMR spectra of $Mn(BrQ)_3$ in $CDCl_3$ at 273 K: (a) 5-H signals; (b) 3-H signals; (c) 6-H signals.

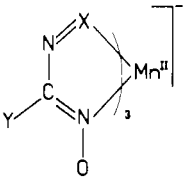

2 X = NPh, Y = Ph

3 X = O, Y = Et

The $Mn(RQ)_3$ system constitutes the first example of low-spin manganese(III) in a nonporphyrinic O,N environment. Certain features in the EPR spectrum of the S_2 state of photosystem II require the presence of a spin-triplet site.[23] Low-spin manganese(III) was a very remote option, since it was unknown in the nonporphyrinic O,N environment which characterizes PS II manganese.[24] The $Mn(RQ)_3$ results show that the said option cannot be summarily rejected.

b. Role of Oximato Chelation. In RQ^- we have the first example of a chelating ligand system that has afforded tractable low-spin complexes of both di- and trivalent manganese. Thus far, only monodentate CN^- was known to have this ability. The strong-field nature of RQ^- is believed to arise primarily from five-membered oximato nitrogen chelation—a feature also present in **2** and **3**. The non-oxime donor function in the chelate varies considerably in this group: quinone oxygen in $Mn(RQ)_3^-$, azo nitrogen in **2**, and nitroso oxygen in **3**. Other instances of relatively large ligand field splitting via oximato nitrogen chelation have been documented.[25]

C. Isomeric Structure. a. ^1H NMR and Meridional Geometry of $Mn(RQ)_3$. Single crystals of $Mn(RQ)_3$ could not be grown,

(15) As shown later, the solution actually contains both *mer* and *fac* isomers. The observed six-line spectra indicate that the isotropic average g and A parameters are the same for the two isomers within experimental error. Frozen-solution (77 K) spectra are complex with many lines, as would be expected for an isomeric mixture.

(16) Griffith, W. P. *Coord. Chem. Rev.* **1975**, *17*, 177–247. Cooke, A. M.; Duffes, H. *J. Proc. Phys. Soc., A* **1955**, *68*, 32.
(17) Landrum, J. T.; Hatano, K.; Scheidt, W. R.; Reed, C. A. *J. Am. Chem. Soc.* **1990**, *102*, 6729–6735.
(18) Hansen, A. P.; Goff, H. M. *Inorg. Chem.* **1984**, *23*, 4519–4525.
(19) Figgis, B. N. *Trans. Faraday Soc.* **1961**, *57*, 204–209.
(20) (a) Cotton, F. A.; Monchamp, R. R.; Henry, R. J. M.; Young, R. C. *J. Inorg. Nucl. Chem.* **1959**, *10*, 28–38. (b) Jakob, W.; Senkowski, T. *Rocz. Chem.* **1964**, *38*, 1751. (c) Monoharan, P. T.; Gray, H. B. *Chem. Commun.* **1965**, 324–325.
(21) Connelly, N. G.; Hassard, K. A.; Dunne, B. J.; Orpen, A. G.; Raven, S. J.; Carriedo, G. A.; Riera, V. *J. Chem. Soc., Dalton Trans.* **1988**, 1623–1629.
(22) Couzerh, P.; Jeannin, Y.; Rocchicioli-Deltcheff, C.; Valentini, F. *J. Coord. Chem.* **1979**, *6*, 221–233.
(23) de Paula, J. C.; Brudrig, G. W. *J. Am. Chem. Soc.* **1985**, *107*, 2643–2648.
(24) (a) Kirby, J. A.; Robertson, A. S.; Smith, J. P.; Thompson, A. C.; Cooper, S. R.; Klein, M. P. *J. Am. Chem. Soc.* **1981**, *103*, 5529–5537. (b) Guiles, R. D.; Zimmerman, J. L.; McDermott, A. E.; Yachandra, V. K.; Cole, J. L.; Dexheimer, S. L.; Britt, R. D.; Wieghardt, K.; Bossek, U.; Sauer, K.; Klein, M. P. *Biochemistry* **1990**, *29*, 471–485. (c) Yachandra, V. K.; Guiles, R. D.; McDermott, A. E.; Britt, R. D.; Dexheimer, S. L.; Sauer, K.; Klein, M. P. *Biochim. Biophys. Acta* **1986**, *850*, 324–332. (d) Tamura, N.; Ikenuchi, M.; Inone, Y. *Biochim. Biophys. Acta* **1989**, *973*, 281–289.

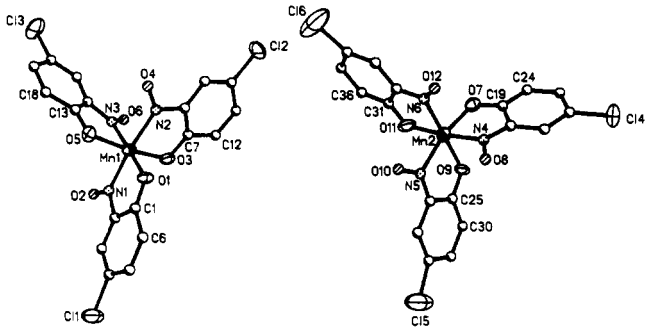

Figure 3. Views of *mer*-$Mn(ClQ)_3^-$ and *fac*-$Mn(ClQ)_3^-$.

but ^1H NMR data unequivocally prove their isomeric nature. The contact-shifted spectrum of $Mn(BrQ)_3$ shown in Figure 2 is representative of the entire family. Chemical shift data, including the expected inverse dependence on absolute temperature[26] for one case, have been deposited as supplementary material (Table SII).

Three equally intense signals are systematically observed for each of the three (3-H, 5-H, 6-H) types of ring protons.[27] This signifies *mer* geometry, **4** (C_1 symmetry, inequivalent ligands),

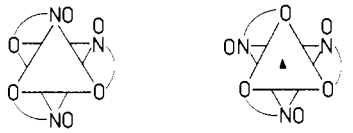

4 **5**

as opposed to *fac* geometry, **5** (C_3 symmetry, equivalent ligands).[1,3,28] The equilibrium concentration of the *fac* form is unobservably small. This finding is consistent with electrochemical results; vide infra.

b. X-ray Crystallography of $[Et_4N][Mn(ClQ)_3]$. The crystal lattice consists of an ordered arrangement of equal proportions of *mer* and *fac* isomers, the formula of the asymmetric unit being $[Et_4N]_2[mer\text{-}Mn(ClQ)_3][fac\text{-}Mn(ClQ)_3]$. Views of the two isomers along with the atom-numbering schemes are depicted in Figure 3. Selected bond parameters are listed in Table II. The complex diffracted relatively weakly, and the diffraction peaks were broad. Only moderate precision could therefore be achieved for the derived bond parameters. For this reason, comparisons and comments will be limited to gross features only.

The ClQ ligands are chelated in the N,O fashion, and each of the five-membered chelate rings is satisfactorily planar (mean deviation ≤0.05 Å). The C–O, C–N, and N–O distances are comparable with those in other RQ complexes,[29] including ferroverdin.[5a] A significant nitrosophenolate resonance contribution is probably present.[29c]

The Mn–N and Mn–O distances in pseudooctahedral high-spin ($S = {}^5/_2$) manganese(II) complexes usually fall in the range 2.1–2.3 Å. Only two of the metal–ligand distances in $Mn(ClQ)_3^-$ are marginally larger than 2 Å: Mn(2)–O(11), 2.012 (14) Å; Mn(2)–O(9), 2.096 (13) Å. All the other distances lie below 2 Å. The average Mn–N distance in $Mn(ClQ)_3^-$ is 1.93 (2) Å; that in the anionic low-spin manganese(II) (arylazo)oximate **2** is 1.95 (2) Å.[11] There is significant contraction of the manganese(II) atom upon spin-pairing.[30]

Table II. Selected Bond Distances and Angles in $[Et_4N][Mn(ClQ)_3]$

Distances, Å			
Mn(1)–O(1)	1.963 (11)	Mn(2)–O(7)	1.945 (12)
Mn(1)–O(3)	1.920 (11)	Mn(2)–O(9)	2.096 (13)
Mn(1)–O(5)	1.910 (11)	Mn(2)–O(11)	2.012 (14)
Mn(1)–N(1)	1.911 (15)	Mn(2)–N(4)	1.947 (16)
Mn(1)–N(2)	1.961 (13)	Mn(2)–N(5)	1.934 (17)
Mn(1)–N(3)	1.950 (14)	Mn(2)–N(6)	1.902 (19)
O(1)–C(1)	1.244 (20)	O(7)–C(19)	1.310 (21)
O(3)–C(7)	1.304 (20)	O(9)–C(25)	1.220 (24)
O(5)–C(13)	1.254 (20)	O(11)–C(31)	1.272 (24)
N(1)–O(2)	1.232 (20)	N(4)–O(8)	1.287 (19)
N(2)–O(4)	1.268 (16)	N(5)–O(10)	1.243 (23)
N(3)–O(6)	1.277 (17)	N(6)–O(12)	1.220 (27)
Angles, deg			
O(1)–Mn(1)–O(3)	92.8 (5)	O(7)–Mn(2)–O(9)	85.7 (5)
O(1)–Mn(1)–O(5)	94.0 (5)	O(7)–Mn(2)–O(11)	92.7 (5)
O(3)–Mn(1)–O(5)	171.7 (5)	O(9)–Mn(2)–O(11)	91.7 (5)
O(1)–Mn(1)–N(1)	82.1 (6)	O(7)–Mn(2)–N(4)	82.5 (5)
O(1)–Mn(1)–N(2)	94.0 (5)	O(7)–Mn(2)–N(5)	166.6 (6)
O(1)–Mn(1)–N(3)	174.2 (5)	O(7)–Mn(2)–N(6)	92.3 (6)
O(3)–Mn(1)–N(1)	92.4 (5)	O(9)–Mn(2)–N(4)	89.7 (5)
O(3)–Mn(1)–N(2)	81.9 (5)	O(9)–Mn(2)–N(5)	81.6 (6)
O(3)–Mn(1)–N(3)	92.3 (5)	O(9)–Mn(2)–N(6)	175.4 (6)
O(5)–Mn(1)–N(1)	93.2 (6)	O(11)–Mn(2)–N(4)	174.8 (6)
O(5)–Mn(1)–N(2)	93.0 (5)	O(11)–Mn(2)–N(5)	91.9 (7)
O(5)–Mn(1)–N(3)	80.7 (5)	O(11)–Mn(2)–N(6)	82.4 (7)
N(1)–Mn(1)–N(2)	173.0 (6)	N(4)–Mn(2)–N(5)	93.2 (7)
N(1)–Mn(1)–N(3)	100.3 (6)	N(4)–Mn(2)–N(6)	94.1 (7)
N(2)–Mn(1)–N(3)	84.1 (6)	N(5)–Mn(2)–N(6)	100.7 (8)

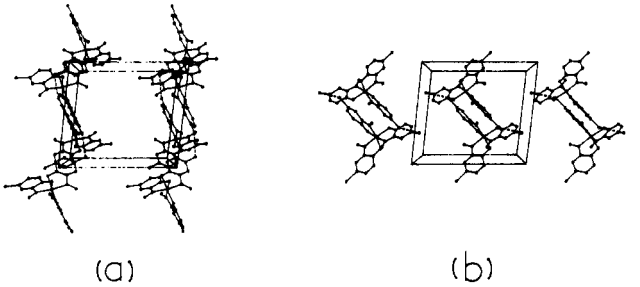

Figure 4. Packing diagrams (down the *c* axis) for (a) *mer*-$Mn(ClQ)_3^-$ and (b) *fac*-$Mn(ClQ)_3^-$ in the lattice of $[Et_4N][Mn(ClQ)_3]$.

Nonbonded Cl···Cl interactions dominate crystal packing. The interactions are limited to molecules of the same isomeric type. The *mer*···*mer* interactions, 3.548 (6) Å, occur for Cl(2) and Cl(3) atoms and extend through the lattice as shown in the packing diagram of Figure 4a. On the other hand, the *fac*···*fac* interactions, 3.555 (8) Å, involve Cl(5) and Cl(6) atoms in pairs of molecules which pack as in Figure 4b.

D. Redox and Isomerization Equilibria. The main result of the previous section is that the trivalent state strongly prefers the *mer* geometry but the bivalent state is compatible with both *mer* and *fac* geometries. Electrochemical results fully corroborate this and go further to quantitate redox and isomerization equilibria. Variable-temperature (230–298 K) voltammetry was performed at a platinum electrode in dichloromethane and acetonitrile solutions. Selected reduction potential and coulometric data are collected in Table III, and representative voltammograms are displayed in Figures 5 and 6. All potentials are referenced to the saturated calomel electrode, SCE.

(25) Mohanty, J. G.; Singh, R. P.; Chakravorty, A. *Inorg. Chem.* **1975**, *14*, 2178–2183.
(26) La Mar, G. N.; Dew, W., Jr.; Holm, R. H. *NMR of Paramagnetic Molecules*; Academic: New York, 1973.
(27) The conclusion regarding isomer geometry is not dependent on the assignment of signals to specific protons, since nine equally intense signals are observed for the three ring protons. The assignments shown in Figure 3 are based on comparison with the spectra of disubstituted complexes such as $Mn(4,6\text{-}Me_2Q)_3$ (6-H signal absent) and $Mn(4,5\text{-}Me_2Q)_3$ (5-H signal absent).
(28) (a) Fay, R. C.; Piper, T. S. *J. Am. Chem. Soc.* **1962**, *84*, 2304–2308. (b) Chakravorty, A.; Holm, R. H. *Inorg. Chem.* **1964**, *3*, 1521–1524. (c) Kalia, K. C.; Chakravorty, A. *Inorg. Chem.* **1969**, *8*, 2586–2590.
(29) (a) Bisi Castellani, C.; Carugo, O.; Coda, A. *Acta Crystallogr.* **1988**, *C44*, 267–270. (b) Bisi Castellani, C.; Carugo, O.; Coda, A. *Inorg. Chem.* **1987**, *26*, 671–675. (c) Carugo, O.; Djinovic, K.; Rizzi, M.; Bisi Castellani, C. *J. Chem. Soc., Dalton Trans.* **1991**, 1255–1258 and references therein.
(30) Shannon, R. D.; Prewitt, C. T. *Acta Crystallogr.* **1969**, *B25*, 925–946. Shannon, R. D. *Acta Crystallogr.* **1976**, *A32*, 751–767.

Table III. Electrochemical Data[a-c]

compd	solvent	temp, K	cyclic voltammetric data: *mer* E_{pa}, V	*mer* E_{pc}, V	*mer* $E°$, V (ΔE_p, mV)	*fac* E_{pa}, V	*fac* E_{pc}, V	*fac* $E°$, V (ΔE_p, mV)	n (E, V)
$Mn^{III}(ClQ)_3$	CH_2Cl_2	260	+0.48	+0.28	+0.38 (200)	+0.58	*d*		0.95 (0.0)
		298	+0.44	+0.22	+0.33 (220)				1.04 (0.0)
	CH_3CN	260	+0.46	+0.38	+0.42 (80)				1.08 (0.0)
		298	+0.45	+0.37	+0.41 (80)				0.97 (0.0)
$Mn^{II}(ClQ)_3^-$	CH_2Cl_2	260	+0.44	+0.28	+0.36 (160)	+0.58	+0.49	+0.54 (90)	0.95 (0.80)
		298	+0.44	+0.26	+0.35 (180)				1.02 (0.80)
	CH_3CN	260	+0.48	+0.38	+0.43 (100)				0.96 (0.80)
		298	+0.48	+0.38	+0.43 (100)				0.98 (0.80)
$Mn^{III}(BrQ)_3$	CH_2Cl_2	298	+0.42	+0.27	+0.35 (150)				0.99 (0.0)
	CH_3CN	298	+0.46	+0.40	+0.43 (60)				1.03 (0.0)
$Mn^{II}(BrQ)_3^-$	CH_2Cl_2	260	+0.43	+0.31	+0.37 (120)	+0.58	+0.50	+0.54 (80)	0.98 (0.80)
		298	+0.47	+0.26	+0.37 (210)				1.03 (0.80)
$Mn^{III}(MeQ)_3$	CH_2Cl_2	298	+0.19	+0.02	+0.11 (170)				0.96 (-0.2)
	CH_3CN	298	+0.23	+0.15	+0.19 (80)				0.98 (-0.2)
$Mn^{II}(MeQ)_3^-$	CH_2Cl_2	260	+0.19	+0.01	+0.10 (180)	+0.31	+0.23	+0.27 (70)	0.98 (0.60)
		298	+0.18	+0.02	+0.10 (160)				1.04 (0.60)
$Mn^{III}(^tBuQ)_3$	CH_2Cl_2	298	+0.18	+0.04	+0.11 (140)				0.99 (-0.2)
	CH_3CN	298	+0.22	+0.14	+0.18 (80)				1.09 (0.0)
$Mn^{II}(^tBuQ)_3^-$	CH_2Cl_2	260	+0.23	+0.01	+0.12 (220)	+0.34	+0.26	+0.30 (80)	0.94 (0.60)
		298	+0.22	0.00	+0.11 (220)				0.98 (0.60)
	CH_3CN	260	+0.25	+0.17	+0.21 (80)	+0.38	*d*		1.05 (0.60)
		298	+0.24	+0.16	+0.20 (80)				0.99 (0.60)

[a] At a platinum disk electrode; supporting electrolyte tetraethylammonium perchlorate (TEAP, 0.1 M); scan rate 50 mV s^{-1}; reference electrode SCE; solute concentration $\sim 10^{-3}$ M. [b] Meaning of symbols: E_{pa}, anodic peak potential; E_{pc}, cathodic peak potential; $\Delta E_p = E_{pa} - E_{pc}$, $E° = {}^1/_2(E_{pa} + E_{pc})$; $n = Q/Q'$ where Q is the observed Coulomb count for constant-potential coulometry at E volt and Q' is the calculated Coulomb count. [c] Responses not observable in CH_3CN at any of the two temperatures for $Mn(RQ)_3$. [d] Cathodic peak poorly developed/not developed.

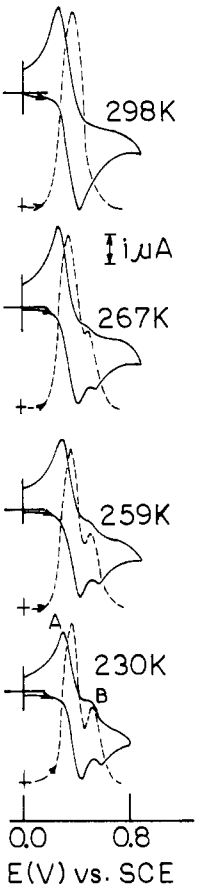

Figure 5. Variable-temperature cyclic (—) and differential pulse (- - -) voltammograms of a $\sim 10^{-3}$ M $Mn(ClQ)_3^-$ solution in CH_2Cl_2 (0.1 M TEAP) at a platinum electrode with scan rates of 50 mV s^{-1} (CV) and 10 mV s^{-1} (DPV) and a modulation amplitude (DPV) of 25 mV. The marked current range is 10 μA (CV) or 5 μA (DPV). The voltammograms were run for the same solution except for that at 230 K.

a. $Mn(RQ)_3^-$. In cold solutions two cyclic responses (A and B; Figure 5) of unequal heights are seen, the smaller response being B, which is better observed in dichloromethane than in acetonitrile (Table III). Upon warming, B progressively loses definition, and at 298 K, only A survives. Coulometric oxidation at potentials above the anodic peak of B corresponds to the net transfer of one electron throughout the temperature range.

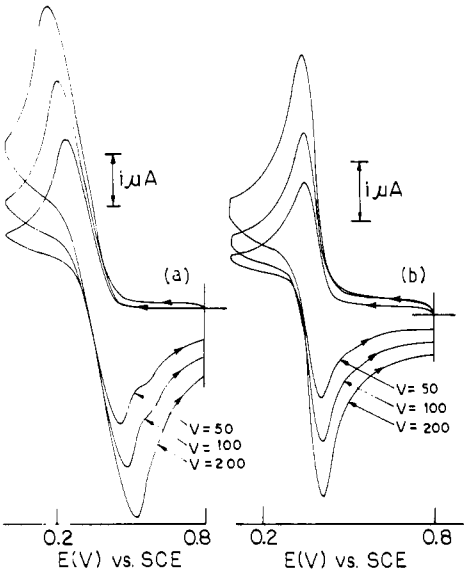

Figure 6. Variable scan rate (v, mV s^{-1}) cyclic voltammograms of 10^{-3} M $Mn(ClQ)_3$ in (a) dichloromethane (0.1 M TEAP) at 263 K and (b) acetonitrile (0.1 M TEAP) at 256 K at a platinum electrode. The marked current range is 10 μA.

The results taken collectively with those of $Mn(RQ)_3$ reported below can be rationalized in terms of the redox and isomerization equilibria of eqs 1–4. The responses A and B correspond to the *mer* (eq 1) and *fac* (eq 2) couples, respectively.

Values of K^{II} (eq 3) were calculated from anodic peak heights of differential pulse voltammograms, and the results at 260 K (peaks are still well-separated at this temperature) are collected in Table IV. The equilibrium abundance of the *mer* isomer is 2–3 times that of the *fac* form, and it appears to increase with temperature. The 1:1 *mer*:*fac* ratio in crystalline $[Et_4N]$-

Table IV. Equilibrium Constants at 260 K (CH_2Cl_2 Solvent)

R	K^{II} [a]	$10^{-3}K^{III}$ [b]	$10^{-3}K^{cr}$ [c]	R	K^{II} [a]	$10^{-3}K^{III}$ [b]	$10^{-3}K^{cr}$ [c]
Cl	2.5	7.8	3.1	Me	2.4	4.8	2.0
Br	2.4	4.8	2.0	^{t}Bu	2.1	6.5	3.1

[a] From differential-pulse voltammetry. [b] Computed from eq 5 and Table V. [c] $K^{cr} = K^{III}/K^{II}$.

$$mer\text{-}Mn^{III}(RQ)_3 + e^- \overset{E^\circ(mer)}{\rightleftharpoons} mer\text{-}Mn^{II}(RQ)_3^- \quad (1)$$

$$fac\text{-}Mn^{III}(RQ)_3 + e^- \overset{E^\circ(fac)}{\rightleftharpoons} fac\text{-}Mn^{II}(RQ)_3^- \quad (2)$$

$$fac\text{-}Mn(RQ)_3^- \overset{K^{II}}{\rightleftharpoons} mer\text{-}Mn(RQ)_3^- \quad (3)$$

$$fac\text{-}Mn(RQ)_3 \overset{K^{III}}{\rightleftharpoons} mer\text{-}Mn(RQ)_3 \quad (4)$$

$[Mn(ClQ)_3]$ is a special situation stabilized by lattice forces and does not correspond to any particular solution equilibrium condition.

The unstable *fac*-$Mn(RQ)_3$ isomer formed by stereoretentive electrooxidation of *fac*-$Mn(RQ)_3^-$ survives on the cyclic voltammetric time scale, particularly in cold dichloromethane (Figure 5). Upon warming, homogeneous isomerization to *mer*-$Mn(RQ)_3$ (eq 4, forward reaction) is accelerated and the cathodic peak height of the *fac* couple progressively diminishes. From current ratios of the couple B the rate constant of the homogeneous isomerization process is estimated[31] to lie in the range 0.02–0.04 s^{-1} at 260 K in dichloromethane. The process is more facile in acetonitrile (anodic B response virtually absent) than in dichloromethane (Figure 5).

Values of K^{III} have been estimated with the help of eq 5, which is derived from a cycle interlinking eqs 1–4. Data are given in

$$\begin{array}{ccc} fac\text{-}Mn^{II}(RQ)_3^- & \overset{K^{II}}{\rightleftharpoons} & mer\text{-}Mn^{II}(RQ)_3^- \quad (3) \\ E^\circ(fac)\downarrow\uparrow & & E^\circ(mer)\downarrow\uparrow \\ fac\text{-}Mn^{III}(RQ)_3 & \overset{K^{III}}{\rightleftharpoons} & mer\text{-}Mn^{III}(RQ)_3 \quad (4) \end{array}$$

Table IV, which also includes the cross-reaction (eq 6) constant

$$K^{III} = K^{II} \exp[F/RT\{E^\circ(fac) - E^\circ(mer)\}] \quad (5)$$

$$fac\text{-}Mn(RQ)_3 + mer\text{-}Mn(RQ)_3^- \overset{K^{cr}}{\rightleftharpoons} fac\text{-}Mn(RQ)_3^- + mer\text{-}Mn(RQ)_3 \quad (6)$$

K^{cr} ($=K^{III}/K^{II}$). The K^{III} values are of the order of $\sim 10^4$. Equilibrated solutions of $Mn(RQ)_3$ should thus contain the *mer* isomer in virtually pure form. This is fully consistent with the NMR results already described and with electrochemical behavior of $Mn(RQ)_3$ (see below).

b. $Mn(RQ)_3$. Here a single cathodic peak (*mer* couple) is seen (Figure 6) throughout the temperature range, corroborating that the equilibrium concentration of *fac*-$Mn(RQ)_3$ is negligibly small. On scan reversal in cold solutions, *mer*- and *fac*-$Mn(RQ)_3^-$ become observable as major and minor anodic peaks, respectively. Evidently, the *fac*-$Mn(RQ)_3^-$ isomer arises (eq 3, backward reaction) by isomerization of electrogenerated (eq 1, cathodic scan) *mer*-$Mn(RQ)_3^-$. As the scan rate is increased, the relative height of the minor anodic peak actually decreases, since the time window[32] available for isomerization becomes smaller. In the case of $Mn(ClQ)_3$, the minor peak is virtually unobservable at scan rates >200 mV s^{-1} (time window <0.1 s) at 260 K in dichloromethane. In acetonitrile solution, isomerization occurs faster (Figure 6).

Coulometric reduction of $Mn(RQ)_3$ solutions at potentials below the cathodic peak potential leads to consumption of one electron (Table III) and quantitative generation of $Mn(RQ)_3^-$. Such reduced solutions were used for magnetic and other studies on $Mn(RQ)_3^-$, and it is from such a solution that crystalline $[Et_4N][Mn(ClQ)_3]$ was isolated; vide supra.

Table V. Crystallographic Data for $[Et_4N][Mn(ClQ)_3]$

empirical formula	$C_{26}H_{29}N_4O_6Cl_3Mn$	Z	4
fw	654.8	T, °C	296
space group	$P\bar{1}$	λ, Å	0.710 73
a, Å	12.205 (6)	ρ_{calcd}, g cm^{-3}	1.457
b, Å	13.645 (9)	μ, cm^{-1}	7.39
c, Å	18.076 (10)	transm coeff[a]	0.8979/1
α, deg	91.04 (5)	R,[b] %	8.80
β, deg	94.07 (4)	R_w,[c] %	8.88
γ, deg	96.06 (4)	GOF[d]	1.16
V, Å^3	2985 (3)		

[a] Maximum value normalized to 1. [b] $R = \sum||F_o| - |F_c||/\sum|F_o|$. [c] $R_w = [\sum w(|F_o| - |Fc|)^2/\sum w|F_o|^2]^{1/2}$; $w^{-1} = \sigma^2(|F_o| + g|F_o|^2)$; $g = 0.0002$. [d] The goodness of fit is defined as $[w(|F_o| - |F_c|)^2/(n_o - n_v)]^{1/2}$ where n_o and n_v denote the numbers of data and variables, respectively.

Coulometric reduction of $Mn(RQ)_3$ solutions at potentials below the cathodic peak potential leads to consumption of one electron (Table III) and quantitative generation of $Mn(RQ)_3^-$. Such reduced solutions were used for magnetic and other studies on $Mn(RQ)_3^-$, and it is from such a solution that crystalline $[Et_4N][Mn(ClQ)_3]$ was isolated; vide supra.

c. Trends: Comparison with Other $M(RQ)_3^z$ Complexes. For a given isomer, the R substituent in $Mn(RQ)_3^z$ has the expected effect. Thus the R = Cl complex has higher (by ~300 mV) E° than the R = Me complex. For a given R, $E^\circ(fac)$ is more positive than $E^\circ(mer)$ by ~180 mV (Table III).

The inequality $E^\circ(fac) > E^\circ(mer)$ relates by eq 5 to the inequality $K^{III} > K^{II}$. The *mer* form is sterically more favorable than the *fac* form, in which the pendant oximato oxygen atoms lie closer (compare **4** and **5**). Due to oxidative contraction of metal size,[30] the steric factor is stronger for the trivalent complex. The expected qualitative result is $K^{III} > K^{II}$ and hence $E^\circ(fac) > E^\circ(mer)$. This qualitative trend applies not only to $Mn(RQ)_3^z$ but also to $Fe(RQ)_3^z$ (R = Me, $K^{II} = 4 \times 10^{-3}$, $K^{III} = 6.5$ at 298 K in MeCN)[1] and $Ni(RQ)_3^z$ (R = Me, $K^{II} = 0.87$, $K^{III} = 43$ at 298 K in MeCN).[3]

For a purely satistical ligand distribution, the relation $K^{II} = K^{III} = 3$ should hold. Observed K^{III} values are systematically larger than 3, in agreement with the steric factor being an important contributor. The K^{II} values are however usually smaller than 3, suggesting preferential electrostatic/electronic stabilization of the divalent *fac* isomer. In *fac*-$M^{II}(RQ)_3^-$, the anionic charge is localized on one face of the octahedron; in *mer*-$M^{II}(RQ)_3^-$, it is meridionally spread out. Consequently, electrostatic anion–cation and anion–solvent stabilizing interactions would be stronger in the *fac* isomer, leading to $K^{II} < 3$. In $Fe^{II}(MeQ)_3^-$, K^{II} is unusually low. In this low-spin d^6 situation, the stabilizing π-back-bonding effect would be prevelent particularly strongly in the *fac* form.[33,34] If this d^6-specific effect is indeed important, K^{III} might become unusually low in $Co^{III}(RQ)_3$. Preliminary results[35] support this contention, and further studies, including those on other 3d $M(RQ)_3^z$ species, are in progress.

E. Concluding Remarks. The main findings of this work will now be summarized. The synthesis and characterization of the $Mn(RQ)_3^z$ (R = Cl, Br, Me, ^{t}Bu; z = 1–, 0) family have been achieved. The family has some unique features and represents several firsts in manganese chemistry: (i) a chelating ligand class

(31) Nicholson, R. S.; Shain, I. *Anal. Chem.* **1964**, *36*, 706–723.
(32) Bard, A. J.; Faulkner, L. R. *Electrochemical Methods: Fundamentals and Applications*; John Wiley & Sons: New York, 1980; p 435.
(33) Bursten, B. E. *J. Am. Chem. Soc.* **1982**, *104*, 1299–1304.
(34) Examples of $E^\circ(fac) > E^\circ(mer)$ for d^5–d^6 redox couples are known in substituted carbonyl complexes: Bond, A. M.; Carr, S. W.; Colton, R. *Inorg. Chem.* **1984**, *23*, 2343–2350. Bond, A. M.; Colton, R.; Kevekordes, J. E. *Inorg. Chem.* **1986**, *25*, 749–756.
(35) In $Co(MeQ)_3$, K^{III} has been estimated to be <1 from ^{1}H NMR data: Basu, P. Unpublished results.

Table VI. Atomic Coordinates ($\times 10^4$) and Equivalent[a] Isotropic Displacement Coefficients ($Å^2 \times 10^3$) for $[Et_4N][Mn(ClQ)_3]$

	x	y	z	U(eq)		x	y	z	U(eq)
Mn(1)	−2268 (2)	519 (2)	1288 (2)	43 (1)	C(13)	−4327 (14)	−431 (11)	1179 (9)	39 (5)
Mn(2)	2526 (3)	3894 (2)	3266 (2)	62 (1)	C(14)	−4188 (14)	−150 (11)	1941 (9)	38 (5)
Cl(1)	−1595 (6)	4028 (4)	−1264 (3)	102 (3)	C(15)	−4919 (17)	−437 (14)	2502 (11)	63 (6)
Cl(2)	704 (5)	−1968 (5)	3761 (3)	100 (3)	C(16)	−5852 (17)	−996 (14)	2246 (11)	61 (6)
Cl(3)	−6843 (5)	−1486 (6)	2827 (4)	114 (3)	C(17)	−6103 (17)	−1272 (14)	1457 (11)	66 (6)
Cl(4)	−1964 (5)	5978 (4)	1946 (3)	90 (3)	C(18)	−5352 (17)	−951 (13)	940 (11)	59 (6)
Cl(5)	6634 (7)	7637 (5)	3280 (7)	177 (5)	C(19)	587 (14)	3845 (12)	2422 (9)	41 (5)
Cl(6)	2814 (13)	167 (6)	5608 (5)	245 (8)	C(20)	643 (14)	4756 (11)	2847 (9)	36 (5)
O(1)	−1388 (9)	475 (8)	423 (6)	50 (5)	C(21)	−112 (15)	5421 (12)	2687 (9)	45 (5)
O(2)	−3057 (10)	2378 (9)	1197 (6)	60 (4)	C(22)	−937 (16)	5154 (13)	2157 (10)	54 (5)
O(3)	−1019 (10)	1062 (8)	1928 (6)	56 (5)	C(23)	−1081 (16)	4238 (14)	1774 (10)	57 (5)
O(4)	−2253 (10)	−1582 (8)	1488 (6)	56 (3)	C(24)	−316 (15)	3597 (12)	1927 (9)	47 (5)
O(5)	−3579 (9)	−120 (8)	775 (6)	53 (5)	C(25)	3856 (19)	5205 (16)	2566 (13)	84 (7)
O(6)	−2983 (10)	836 (9)	2748 (7)	65 (4)	C(26)	4270 (16)	5359 (13)	3271 (11)	54 (5)
O(7)	1344 (10)	3256 (8)	2588 (6)	59 (5)	C(27)	5204 (24)	6135 (21)	3628 (16)	123 (10)
O(8)	1679 (11)	5665 (9)	3760 (7)	71 (4)	C(28)	5603 (18)	6692 (15)	3058 (13)	68 (6)
O(9)	3134 (9)	4571 (7)	2325 (7)	61 (5)	C(29)	5278 (28)	6592 (23)	2353 (19)	135 (10)
O(10)	3938 (13)	4647 (11)	4431 (9)	107 (5)	C(30)	4472 (25)	5927 (21)	2099 (16)	117 (9)
O(11)	3465 (12)	2779 (8)	3164 (7)	83 (6)	C(31)	3236 (17)	2231 (14)	3705 (11)	67 (6)
O(12)	1345 (15)	3470 (12)	4500 (10)	115 (6)	C(32)	2530 (18)	2368 (15)	4242 (12)	70 (6)
N(1)	−2514 (12)	1782 (10)	910 (8)	48 (4)	C(33)	2262 (23)	1767 (20)	4857 (15)	116 (9)
N(2)	−1821 (11)	−721 (9)	1681 (7)	47 (4)	C(34)	2952 (21)	935 (17)	4906 (14)	90 (7)
N(3)	−3240 (11)	452 (9)	2101 (7)	45 (4)	C(35)	3567 (23)	835 (19)	4354 (16)	107 (9)
N(4)	1503 (13)	4889 (11)	3334 (8)	63 (5)	C(36)	3844 (24)	1367 (21)	3756 (16)	121 (9)
N(5)	3749 (16)	4737 (13)	3752 (10)	89 (6)	C(37)	6596 (21)	2588 (18)	4286 (14)	104 (8)
N(6)	1997 (16)	3180 (13)	4086 (10)	88 (6)	C(38)	6511 (22)	2454 (18)	5108 (14)	105 (8)
N(7)	7405 (12)	3361 (10)	4050 (8)	53 (4)	C(39)	8528 (26)	3165 (22)	4272 (16)	136 (11)
N(8)	2937 (12)	2559 (10)	655 (7)	52 (4)	C(40)	8911 (21)	2190 (18)	4061 (13)	98 (8)
C(1)	−1392 (15)	1235 (12)	53 (10)	46 (5)	C(41)	7368 (22)	3303 (18)	3217 (14)	103 (8)
C(2)	−1970 (13)	2008 (11)	256 (9)	35 (5)	C(42)	6390 (22)	3647 (18)	2838 (14)	100 (8)
C(3)	−2067 (14)	2860 (12)	−115 (9)	46 (5)	C(43)	7256 (22)	4365 (19)	4366 (14)	111 (9)
C(4)	−1516 (17)	2985 (14)	−733 (11)	66 (6)	C(44)	7945 (24)	5272 (21)	4089 (15)	123 (10)
C(5)	−902 (18)	2253 (15)	−1000 (11)	72 (6)	C(45)	3617 (25)	2692 (21)	−31 (15)	123 (10)
C(6)	−828 (16)	1411 (13)	−637 (10)	56 (5)	C(46)	4480 (30)	3600 (26)	58 (19)	163 (13)
C(7)	−617 (14)	394 (12)	2342 (9)	41 (5)	C(47)	3524 (19)	2542 (16)	1372 (12)	87 (7)
C(8)	−983 (13)	−580 (11)	2234 (9)	33 (4)	C(48)	4299 (24)	1714 (20)	1458 (15)	120 (9)
C(9)	−636 (15)	−1312 (12)	2648 (10)	44 (5)	C(49)	2172 (20)	1683 (17)	489 (13)	92 (7)
C(10)	216 (16)	−1069 (13)	3209 (10)	56 (5)	C(50)	1385 (19)	1277 (16)	1052 (12)	86 (7)
C(11)	676 (17)	−85 (15)	3292 (11)	65 (6)	C(51)	2226 (19)	3397 (16)	741 (12)	81 (7)
C(12)	272 (16)	636 (14)	2903 (11)	56 (5)	C(52)	1456 (26)	3635 (21)	104 (17)	134 (10)

[a] Equivalent isotropic U defined as one-third of the trace of the orthogonalized U_{ij} tensor.

affording tractable low-spin complexes for the metal in both divalent and trivalent states, (ii) the low-spin trivalent state in a nonporphyrinic O,N environment, and (iii) tris chelate geometrical isomerism for the divalent and trivalent states—a phenomenon dramatized in crystalline $[Et_4N][Mn(ClQ)_3]$, where *mer* and *fac* isomers coexist in a 1:1 ratio.

The low-spin nature of $Mn(RQ)_3^z$ is related to oximato chelation. The geometrical isomer preferences of the two oxidation states are very different: the trivalent state is strongly matched to the *mer* geometry, while the divalent state is compatible with both geometries. Isomer concentrations in excess of equilibrium values can be temporarily established via rapid voltammetric electron transfer. The system however recognizes the imbalance promptly, and it is corrected by spontaneous isomerization.

The $Mn(RQ)_3^z$ family is compared with the previously reported $Fe(RQ)_3^z$ and $Ni(RQ)_3^z$ families in terms of isomer preferences. A qualitative rationale regarding the observed trends can be devised on the basis of steric (trivalent *mer*), electrostatic (divalent *fac*), and electronic (d^6 *fac*) factors; the entries in parentheses represent the form specially stabilized by each factor. The net effect in all the three families is $K^{III} > K^{II}$, which requires that the trivalent–divalent metal reduction potentials should follow the order $E°(fac) > E°(mer)$. This inequality is experimentally realized in all three families. The cases of other $M(RQ)_3^z$ families are under scrutiny.

Experimental Section

Materials. The purification of acetonitrile and dichloromethane and the preparation of tetraethylammonium perchlorate (TEAP) for electrochemical work were done as before.[36] For synthetic experiments, commercially available solvents and chemicals were used and $Mn(MeCO_2)_3 \cdot 2H_2O$ was prepared as reported.[37]

Physical Measurements. Spectra were recorded on the following equipment: UV–vis, Hitachi 330 spectrophotometer; X-band EPR, Varian E-109C spectrometer (DPPH standard, $g = 2.0037$); variable-temperature ^1H NMR in $CDCl_3$, Bruker 270-MHz spectrometer (Me_4Si internal standard). Magnetic susceptibility of solids were measured with a Model 155 PAR vibrating-sample magnetometer fitted with a Model L75FBAL Walker Scientific magnet. Solution magnetic moments were determined by Evans' method[38] in dichloromethane or chloroform utilizing the shift of the Me_4Si ^1H signal. Microanalyses (C, H, N) were performed with a Perkin-Elmer Model 240C elemental analyzer.

Electrochemical measurements were done by using the PAR Model 370-4 electrochemistry system incorporating the following: Model 174A polarographic analyzer, Model 175 universal programmer, Model RE0074 X-Y recorder, Model 173 potentiostat, Model 179 digital coulometer, Model 377 cell system. A planar Beckman Model 39273 platinum-inlay working electrode, a platinum-wire auxiliary electrode, and an aqueous saturated calomel reference electrode were used in three-electrode measurements. A platinum-wire-gauge working electrode was used in coulometric measurements. All potentials reported in this work are uncorrected for junction contribution, and all experiments were performed under a nitrogen atmosphere. Measurements in the temperature range 255–298 K were performed with the help of a Haake Model F3-K digital cryostat and circulator connected to jacketed cell bottoms. Measurements at temperatures lower than 255 K were performed by placing the cell

(36) Dutta, D.; Mascharak, P. K.; Chakravorty, A. *Inorg. Chem.* **1981**, *20*, 1673–1679.
(37) Brauer, G., Ed. *Handbook of Preparative Inorganic Chemistry*; Academic Press: New York, 1965; Vol. 2, pp 1469–1470.
(38) Evans, D. F. *J. Chem. Soc.* **1959**, 2003–2005.

bottom in suitable slush baths of liquid nitrogen and a solvent. For example, the 230 K slush bath consisted of MeCN and liquid nitrogen. In all cases, the temperature inside the electrochemical cell was monitored by thermocouples.

Preparation of Complexes. Free ligands were synthesized from phenols via copper complexes according to the procedure of Cronheim.[14] The ligands so synthesized were unstable and were used immediately after preparation. The synthesis of the R = Cl complex is reported here as a representative case. The other complexes were similarly produced in comparative yields by the use of appropriate phenols.

Tris(4-chloro-1,2-benzoquinone 2-oximato)manganese(III), Mn(ClQ)$_3$. To a methanolic solution (15 mL) of 4-chloro-1,2-benzoquinone 2-oxime, HClQ (0.45 g, 2.86 mmol), was added 0.25 g (0.93 mmol) of $Mn(CH_3CO_2)_3 \cdot 2H_2O$, and the mixture was stirred at room temperature for 0.5 h. A dark solid precipitated. It was collected by filtration and then washed thoroughly with methanol and finally with a little water. The product was then dried in vacuo over P_4O_{10}; yield 0.45 g (92%).

Tetraethylammonium Tris(4-chloro-1,2-benzoquinone 2-oximato)manganate(II), [Et$_4$N][Mn(ClQ)$_3$]. A 20-mL solution of $Mn(ClQ)_3$ (0.05 g, 0.095 mmol) in MeCN containing 0.40 g of $[NH_4][PF_6]$ (supporting electrolyte) was subjected to constant-potential coulometric reduction at 0.0 V. The reduction was complete at a count of 9.16 C (the calculated count for one-electron transfer was 9.20 C). The color of the solution changed from brown to green. The solution was then evaporated to dryness in vacuo, and the solid (presumably an ammonium salt of $Mn(ClQ)_3^-$) was extracted with CH_2Cl_2. The extract was filtered, and to the filtrate was added 0.04 g of tetraethylammonium chloride. This solution was then layered with *n*-hexane in a 1:3 ratio. A gummy material deposited which crystallized spontaneously but slowly. The yield was 25 mg (40%). Anal. Calcd for $MnC_{26}H_{29}N_4Cl_3$: C, 47.68; H, 4.43; N, 8.56. Found: C, 47.66; H, 4.53; N, 8.64.

X-ray Structure Determination. The cell parameters of the best available crystal (0.14 × 0.19 × 0.28 mm^3) were determined by a least-squares fit of 20 reflections (2θ = 7–15°) selected from a rotation photograph. Lattice dimensions and the Laue group were checked by axial photography. The crystal system was found to be triclinic. Search for the presence of higher symmetry did not yield positive results. Data were collected by the ω-scan method in the 2θ range 2–43° (it was verified that very few significant reflections occurred at higher angles) on a Nicolet R3m/V diffractometer with graphite-monochromated Mo Kα radiation (λ = 0.710 73 Å). Two check reflections measured after every 98 reflections showed no significant intensity reduction during the 62-h exposure to X-rays. Data were corrected for Lorentz–polarization effects, and an empirical absorption correction was done on the basis of an azimuthal scan of five reflections.[39] Of the 7287 reflections collected, 6847 were unique, of which 2342 satisfying the relation $I > 2.8\sigma(I)$ were used for structure solution.

The metal atoms were located from a Patterson map, and other non-hydrogen atoms emerged from difference Fourier maps. Due to the limited volume of the data set, only manganese, chlorine, and coordinated oxygen atoms were refined anisotropically. The hydrogen atoms were added at calculated positions with fixed U (=0.08 Å^2) in the last cycle of refinement. All refinements were performed by the block-matrix least-squares procedure. The number of parameters refined was 391, and the highest residual peak on a final difference Fourier map was 0.46 e Å^{-3}. All calculations were done on a MicroVAX II computer with the programs of SHELXTL-PLUS.[40] Significant crystal data are listed in Table V. Atomic coordinates and isotropic thermal parameters are collected in Table VI.

Acknowledgment. Crystallography was performed at the National Single Crystal Diffractometer Facility, Department of Inorganic Chemistry, Indian Association for the Cultivation of Science. We are grateful to the Department of Science and Technology, New Delhi, and Council of Scientific and Industrial Research, New Delhi, for financial support. Affiliation with the Jawaharlal Nehru Centre for Advanced Scientific Research, Bangalore, is acknowledged.

Supplementary Material Available: Tables SI and SII, giving analytical data and ^{1}H NMR shifts of $Mn(RQ)_3$ complexes, and Tables SIII–SVI, listing anisotropic thermal parameters, complete bond distances and angles, and hydrogen atom positional parameters (10 pages). Ordering information is given on any current masthead page.

(39) North, A. C. T.; Phillips, D. C.; Matthews, F. S. *Acta Crystallogr.* **1968**, *A24*, 351–359.

(40) Sheldrick, G. M. *SHELXTL PLUS 88, Structure Determination Software Programs*; Nicolet Instrument Corp.: Madison, WI, 1988.